Inorganic Chemistry

pubs.acs.org/IC

Article

Nitric Oxide Oxygenation Reactions of Cobalt-Peroxo and Cobalt-Nitrosyl Complexes

Kulbir, Akshaya Keerthi C. S,[‖] Sulthana Beegam,[‖] Sandip Das, Prabhakar Bhardwaj, Mursaleem Ansari, Kuldeep Singh, and Pankaj Kumar*

Cite This: *Inorg. Chem.* 2023, 62, 7385−7392

Read Online

ACCESS | Metrics & More | Article Recommendations | Supporting Information

ABSTRACT: Here, we report a comparative study of nitric oxide oxidation (NOO) reactions of Co^{III}-peroxo ($Co^{III}-O_2^{2-}$) and Co-nitrosyl ({CoNO}^{8}) complexes bearing the same N_4-donor ligand (HMTETA) framework. In this regard, we prepared and characterized two new $[(HMTETA)Co^{III}(O_2^{2-})]^+$ (**2**, $S = 2$) and $[(HMTETA)Co(NO)]^{2+}$ (**3**, $S = 1$) complexes from $[(HMTETA)Co^{II}(CH_3CN)_2]^{2+}$ (**1**). Both complexes (**2** and **3**) are characterized by different spectroscopic measurements, including their DFT-optimized structures. Complex **2** produces Co^{II}-nitrato $[(HMTETA)Co^{II}(NO_3^-)]^+$ ($Co^{II}-NO_3^-$, **4**) complex in the presence of NO. In contrast, when **3** reacted with a superoxide ($O_2^{\bullet-}$) anion, it generated Co^{II}-nitrito $[(HMTETA)Co^{II}(NO_2^-)]^+$ ($Co^{II}-NO_2^-$, **5**) with O_2 evolution. Experiments performed using $^{18/16}O$-labeled superoxide ($^{18}O_2^{\bullet-}/^{16}O_2^{\bullet-}$) showed that O_2 originated from the $O_2^{\bullet-}$ anion. Both the NOO reactions are believed to proceed via a presumed peroxynitrite (PN) intermediate. Although we did not get direct spectral evidence for the proposed PN species, the mechanistic investigation using 2,4-di-*tert*-butylphenol indirectly suggests the formation of a PN intermediate. Furthermore, tracking the source of the N-atom in the above NOO reactions using ^{15}N-labeled nitrogen (^{15}NO) revealed N-atoms in **4** ($Co^{II}-^{15}NO_3^-$) and **5** ($Co^{II}-^{15}NO_2^-$) derived from the ^{15}NO moiety.

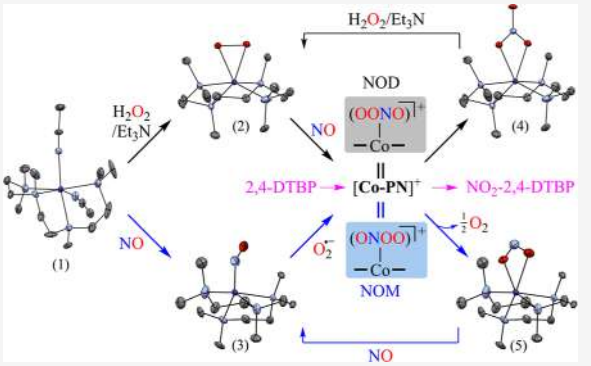

INTRODUCTION

The role of the nitric oxide (NO) molecule in biological systems has seized great interest because it participates in various bio-physiological cascades like cellular transmission, inhibiting vascular smooth muscle cell proliferation, vasodilation, inhibits platelet aggregation, immune response toward various infections, etc.[1] Scantiness of NO in the biological system can cause various ailments such as atherosclerosis,[2] hypertension,[3] atherothrombosis,[4] etc. Hence, optimal NO production becomes essential to maintain biological homeostasis. In this regard, different enzymes participate in the catalytic NO production in humans, bacteria, and plants, i.e., NO synthases[5] and nitrite reductases.[6] NO synthases produce NO via converting L-arginine into L-citrulline.[5] In contrast, nitrite reductase enzymes catalyze the NO production via H^+-mediated reduction of the nitrite moiety under oxygen starvation conditions.[6] However, uncontrolled NO generation leads to different diseases because of the production of different reactive nitrogen species, such as nitrogen dioxide (NO_2) or peroxynitrite (PN), upon reaction with reactive oxygen species (ROS).[7] In this regard, nitric oxide dioxygenase (NOD) helps maintain an optimal level of NO by oxidizing it to bio-friendly nitrate (NO_3^-) via a plausible PN intermediate.[8] In mammals, the NOD reaction is catalyzed by oxyhemoglobin and myoglobin protein, converting excess NO into NO_3^-. While some bacteria with NO reductase and flavodiiron proteins are well known for detoxifying cellular NO by reducing it to nitrous oxide (N_2O).[9]

Mechanistic studies of NOD model systems have been explored to study the NO oxidation reactions. In this regard, different reaction systems have been explored, i.e., (a) NO oxidation reactions via metal−oxygen adducts,[10] and/or (b) reactions of metal−nitrosyls with various ROS (O_2, $O_2^{\bullet-}$, O_2^{2-}, etc.), showing the formation of either NO monooxygenation (NOM) or NO dioxygenation (NOD) products via a plausible M-PN intermediate.[11] Goodwin and co-workers investigated the reaction NO with oxy-coboglobin, showing the formation of $Co-NO_3^-$ at low temperatures.[12] Karlin and co-workers showed the formation of NOD product ($Fe-NO_3^-$) in the reaction of NO with heme-superoxide.[13] Mondal and co-workers also reported the formation of NOD product

Received: February 26, 2023
Published: May 1, 2023

($Co-NO_3^-$) formation when a $Co-O_2^{2-}$ species was reacted with NO.[14] Similarly, Nam and co-workers explored the NOD reaction of $Cr^{IV}-O_2^{2-}$, $Fe^{III}-O_2^{2-}$, and $Fe^{III}-O_2^{\bullet-}$ producing NO_3^- upon reaction with NO.[10d,e,15] The formation of NOM product (NO_2^-) was also observed in various NOO reactions of metal–oxygen adducts with NO, as well as metal–nitrosyl reactions with different ROSs in addition to NO_3^- generation.[10a,11b,16] Nam and co-workers observed NO_2^- formation in the NOO reactions of $Cr^{II}-O_2^{\bullet-}$/or $Mn^{IV}-O_2^{2-}$ and also in the reaction of {CoNO}^{8} with $O_2^{\bullet-}$.[10c,15] Maiti et al. observed formation of NOM product in the NOO reaction of a $Cu^{II}-O_2^{\bullet-}$ via a PN intermediate.[17] In another study, Mondal and co-workers observed $Co^{III}-NO_2^-$ in the reaction of {CoNO}^{8} complexes with $O_2^{\bullet-}$ or H_2O_2.[16] Lehnert and co-workers reported an {CoNO}^{9} which produced $Co-NO_2^-$ and $Co-NO_3^-$ on the reaction with O_2 in the solution phase and solid phase, respectively.[18] Recently, we have compared NOD versus NOM of $Ni^{III}-O_2^{2-}$ and $Co^{III}-O_2^{2-}$ bearing the same ligand framework (12TMC), showing $Ni^{II}-NO_3^-$ and $Co^{II}-NO_2^-$.[10a] It is important to note that NOD and NOM reactions are proposed to proceed via the PN intermediate species.[10−16] The preceding discussion undoubtedly elucidates how the metal centers and the specific starting materials (metal–nitrosyl or metal–oxygen) controls the NOO reaction products (NOM vs NOD) and the reaction intermediates; hence, the mechanism of reactions. Only a handful studies were conducted to explore the role of the metal centers and/or the ligand frameworks, where the metal–nitrosyl[19] or metal–oxygen[20] adducts are explored for NOO reactions.[10c,d,11b,14] Hence, a broad study on several metal–nitrosyl or metal–oxygen adducts is required to establish the detailed mechanism of the NO oxidation to NOM and NOD products.

Herein, we explore the NO oxidation (NOO) reactions of Co^{III}-peroxo and Co-nitrosyl complexes bearing the same N_4-ligand framework. In this regard, $[(HMTETA)Co^{III}(O_2^{2-})]^+$ ($Co^{III}-O_2^{2-}$, **2**)[10a,21] and $[(HMTETA)Co(NO)]^{2+}$ {CoNO}^{8} (**3**)[11,22] (HMTETA = 1,1,4,7,10,10-hexamethyltriethylenetetramine) were prepared from the same initial cobalt complex $[(HMTETA)Co^{II}(CH_3CN)_2]^{2+}$ (**1**) [Supporting Information and Experimental Section (ES), Figure S1] (Scheme 1, reactions a and b). Furthermore, we have explored the reactivity of **2** and **3** with NO and $O_2^{\bullet-}$ (KO_2/18-crown-6), respectively, to follow and identify the NOO reaction products. Complex **2** forms NOD product Co^{II}-nitrato complex, $[(HMTETA)Co^{II}(NO_3^-)]^+$, ($Co^{II}-NO_3^-$, **4**) on reacting with NO (Scheme 1, reaction c) via a plausible *O*-bound PN[10e,15,20a−c] (Co-*O*-PN or Co–OONO) intermediate. While **3** produces NOM product, Co^{II}-nitrito complex, $[(HMTETA)Co^{II}(NO_2^-)]^+$, ($Co^{II}-NO_2^-$, **5**) (Scheme 1, reaction d) via a plausible *N*-bound PN[11b,16,19a−f] (Co-*N*-PN or Co–ONOO). Furthermore, the phenol nitration using the 2,4-DTBP confirms the formation of a proposed PN-intermediate in both NOD and NOM reactions. Mechanistic studies using ^{15}NO showed the formation of $Co^{II}-{}^{15}NO_3^-$ and $Co^{II}-{}^{15}NO_2^-$, confirming that the N-atom came from the NO moiety, while experiments performed using $^{18}O_2^{\bullet-}$ and $^{16}O_2^{\bullet-}$ established that the O-atom of O_2 comes from superoxide anion. In addition, complexes **4** and **5** showed the formation of initial complexes **2** and **3** upon reaction with H_2O_2/Et_3N and NO, respectively (Scheme 1, reactions e and f).

Scheme 1

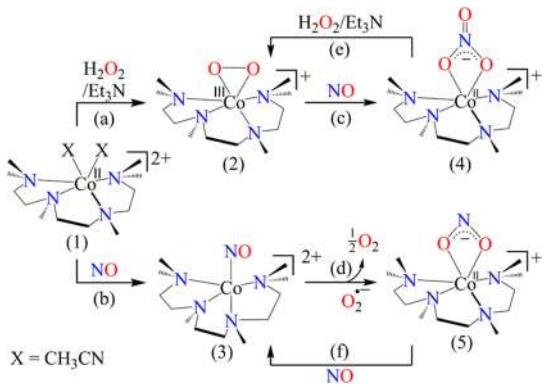

RESULTS AND DISCUSSION

Synthesis of Co^{III}-Peroxo $[(HMTETA)Co^{III}(O_2^{2-})]^+$ (2) and Co-Nitrosyl {CoNO}^{8} (3) Complexes. The primary Co^{III}-peroxo complex, $[(HMTETA)Co^{III}(O_2^{2-})]^+$ (**2**), was prepared by reacting Co^{II}-complex, $[(HMTETA)-Co^{II}(CH_3CN)_2]^{2+}$ (**1**), with a mixture of 5 equiv H_2O_2 and 2.5 equiv Et_3N in CH_3CN at −40 °C (Scheme 1, reaction a; also see Supporting Information & ES).[10a,21] Furthermore, **2** was characterized using various spectroscopic tools, including DFT optimized structure. The UV–vis absorption band of **1** (λ_{max} = 510 nm, ε = 20 M^{-1} cm^{-1}) changed to a new band (λ_{max} = 580 nm, ε = 75 M^{-1} cm^{-1}) upon reaction with H_2O_2 and Et_3N in CH_3CN at −40 °C, suggesting the formation of **2** (Figure 1a, Supporting Information, Figure S2a). The wide

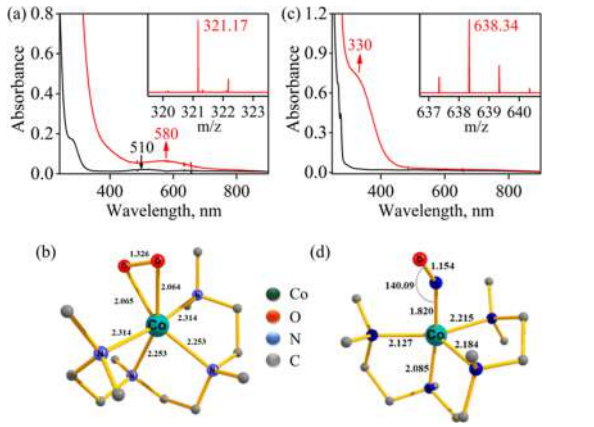

Figure 1. (a) UV–vis spectra of **1** (1 mM, Black line) and **2** (1 mM, red line) in CH_3CN at −40 °C. Inset: isotopic distribution pattern for **2** (red line) and (b) DFT-optimized structures of $^5\mathbf{2}_{hs}$ state. (c) UV–vis spectra of **1** (0.1 mM, black line) and **3** (0.1 mM, Red line) in CH_3CN at −40 °C under an Ar atmosphere. Inset: isotopic distribution pattern for **3** (red line). (d) DFT-optimized structures of $^3\mathbf{3}_{is}$ state.

range ^1H NMR spectrum of **2** confirms a magnetically active Co-ion in the complex **2** (Supporting Information, Figure S2b). Evans method suggested the presence of a high spin Co^{III}-ion (S = 2) in **2** as the calculated magnetic moment was found to be 4.8 BM (Supporting Information, ES and Figure S2c). Electrospray ionization mass spectrum (ESI-MS) of **2** showed a prominent peak at m/z 321.17, and its mass and isotope distribution pattern corresponds to $[(HMTETA)-Co^{III}(O_2^{2-})]^+$ (calcd m/z 321.17) (Figure 1a; Supporting

https://doi.org/10.1021/acs.inorgchem.3c00639
Inorg. Chem. 2023, 62, 7385−7392

Information, Figure S2d). Additionally to the above experimental characterization, the electronic structure of **2** was determined by DFT calculations, suggesting a distorted octahedral geometry with an $S = 2$ ground state (Figure 1b). The Co^{III}-center has an electronic configuration as follows $(\delta_{xy})^1 (\sigma_{z^2}^*)^2 (\pi_{yz}^*)^1 (\pi_{xz}^*)^1 (\sigma_{x^2-y^2}^*)^1$ for the $^5 2_{hs}$ (Supporting Information, Figure S3). The spin density plot suggests that the $\sigma_{z^2}^*$ orbital has two electrons, and the other four orbitals have singly occupied orbitals, i.e., the spin density plot resembles the cubic shape. Meanwhile, Co-peroxo with similar ancillary ligands $[(12TMC)Co(O_2^{2-})]^+$ has been reported to be a low-spin complex and was found to be stable in comparison to **2**.[10a,23]

In addition, we prepared the $\{CoNO\}^8$ (**3**) complex by purging NO gas to the CH_3CN solution of **1** under Ar at −40 °C.[24] UV−visible spectral analysis showed the formation of a new band at λ_{max} = 330 nm (ε = 7000 M^{-1} cm^{-1}) when **1** reacted with NO and was found to be stable for 1 h under Ar at −40 °C (Figure 1c, Supporting Information, Figure S4a). Solution FT-IR spectrum of **1** + NO showed a peak at 1715 cm^{-1}, suggesting a $\{CoNO\}^8$ (**3**), as reported in our previous reports (Supporting Information, Figure S4b).[10a,22,25] ESI-MS spectra showed a peak at 638.34, and its isotopic distribution pattern corresponds to $\{[HMTETA)Co(NO)](BPh_4)\}^+$ (calcd m/z 638.34) (Supporting Information, Figure S4c). ^{1}H NMR spectrum of **2** showed a wide range nice proton signals for the HMTETA ligand (Supporting Information, Figure S4d), confirming a paramagnetic Co-center. To understand the magnetic behavior, we have determined the spin-state of the Co-center in **3** by calculating the magnetic moment using Evans' method and found to be 2.90 BM, proposing a high spin Co-ion ($S = 1$) (Figure S4e). While $\{CoNO\}^8$ with similar ancillary ligands $[(12TMC)Co(NO)]^{2+}$ has been reported to be a low-spin complex with $S = 0$.[11,22c] We attempted to grow the single crystal to determine the structure of **3** but failed even after multiple attempts. Hence, we have performed the DFT calculations to obtain the geometrical details and the spin state. DFT structural analysis showed that **3** is a distorted trigonal bipyramidal (Figure 1d) with an intermediate spin Co-center ($S = 1$), similar to what we observed experimentally. The Co center has an electronic configuration as follows $(\delta_{xy})^2 (\pi_{xz}^*)^1 (\sigma_{x^2-y^2}^*)^1 (\pi_{yz}^*)^2 (\sigma_{z^2}^*)^0$ for the $^3 3_{is}$ (Supporting Information, Figure S5).

NOD Reaction of Co^{III}-Peroxo Complex (2). To follow the NOO reaction of Co^{III}-peroxo species, we reacted **2** with NO to understand the reaction mechanism and determine the reaction products. Upon addition of an equimolar amount of NO (NO saturated CH_3CN solution) to **2**, the typical absorption bands of **2** (λ_{max} = 580 nm) transformed to a new band (λ_{max} = 560 nm), which suggests the formation of a new species (**4**) in CH_3CN at −40 °C under Ar (Figure 2a; Supporting Information, ES, Figure S6). Using various spectroscopic measurements and single-crystal X-ray structural determination (vide infra), complex **4** was determined to be $[(HMTETA)Co^{II}(NO_3^-)]^+$. The FT-IR spectrum of **4** showed a characteristic peak for Co^{II}-bound NO_3^- stretching at 1384 cm^{-1} and shifted to 1350 cm^{-1} ($^{15}NO_3^-$) when **4** was generated in the reaction of ^{15}N-labeled NO and **2** (inset: Figure 3a; Supporting Information, Figure S7a,b), suggesting that the NO_3^- moiety's N-atom is derived from NO ligand. The ESI-MS spectrum of the reaction mixture showed a distinct peak at m/z 351.12, $[(HMTETA)Co^{II}(^{14}NO_3^-)]^+$ (calcd m/z 351.17) (Figure 2b), and shifted to 352.15,

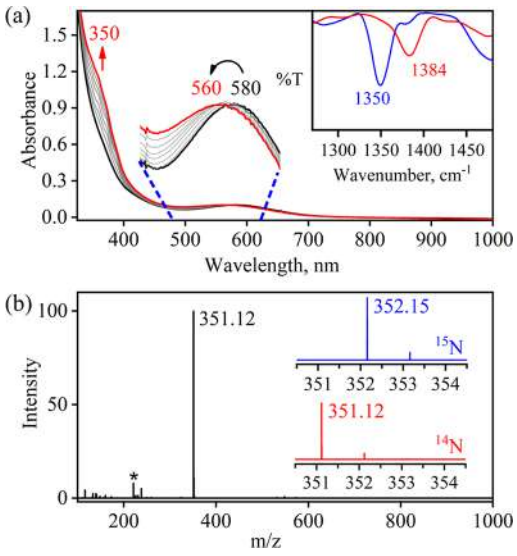

Figure 2. (a) Changes in the UV−vis spectra of **2** (1 mM, black line) when exposed to NO at −40 °C under Ar in CH_3CN. In this reaction, black line (**2**) changed to a red line (**4**). Inset: FT-IR spectra **4**-$^{14}NO_3^-$ (red line) and **4**-$^{15}NO_3^-$ (blue line) recorded in KBr. (b) We observed a peak at 351.12, assigned to $[(HMTETA)-Co^{II}(NO_3^-)]^+$ (calcd m/z 351.17) in the ESI-MS spectrum of **4**. Isotopic distribution patterns for **4**-$^{14}NO_3^-$ (red line) and **4**-$^{15}NO_3^-$ (blue line) shown in the inset.

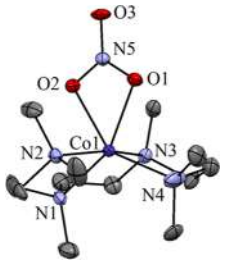

Figure 3. Displacement ellipsoid plot (40% probability) of **4** at 100 K. Anion and H-atoms have been removed for clarity.

$[(HMTETA)Co^{II}(^{15}NO_3^-)]^+$ (calcd m/z 352.17) (inset: Figure 2b; Supporting Information, Figure S8). The ^{1}H NMR suggests a magnetically active Co-center and the same was confirmed using the Evans method, which indicates the presence of a high-spin Co^{II}-center ($S = 3/2$) with a magnetic moment of 3.77 BM (Supporting Information, ES, Figure S9). Using a modified Griess reagent, the yield of NO_3^- formed in the NOD reaction of **2** was determined to be 88 (±2) % (Supporting Information, ES, Figure S10). The UV−vis spectrum of the isolated product of the reaction mixture of **2** + NO was compared with an authentic sample (prepared from **1** + NO_3^-), confirming the formation of **4** (Supporting Information, ES, Figure S11). The final structure details of **4** were confirmed using single-crystal X-ray diffraction, which showed a bidentate NO_3^- coordination to the Co-enter with different Co−O and Co−N bond lengths, contributing to a distorted octahedral geometry (Figure 3, Supporting Information, ES, Figure S12, and Tables T1 and T2).[10a]

As per the previous reports, the NOD reaction of **2** is expected to proceed through the presumed O-bound $[Co\text{-}O\text{-}PN]^+$ intermediate.[10a,e,11,15,20a−c] However, our efforts to follow/characterize it were futile because of its instability. Alternatively, the formation of a PN intermediate in the

https://doi.org/10.1021/acs.inorgchem.3c00639
Inorg. Chem. 2023, 62, 7385−7392

reaction mixture was confirmed by using the DTBP ring-nitration test.[10a,11,16b,19c,k,26] The generation of sufficient amounts of NO_2-2,4-DTBP (2,4-di-*tert*-butyl-6-nitrophenol) and 2,4-DTBP-D (3,3′,5,5′-tetra-*tert*-butyl-[1,1′-biphenyl]-2,2′-diol) (Supporting Information, ES, Figure S13) actively supports the formation of the proposed $[Co\text{-}O\text{-}PN]^+$ intermediate and proposed mechanism of reaction[10e,15,20a−c] in the above reaction (Scheme 2, reactions a and e). In addition, the above reaction was performed in the presence of tetrabutylammonium chloride (TBACl), which showed a higher yield of NO_2-2,4-DTBP [~80 (±2) %], suggesting the release of the PN moiety from Co-center as observed previously (Supporting Information, ES).[19c] Furthermore, we treated **4** with a mixture of H_2O_2 & Et_3N (Scheme 2, reaction c), and the reaction was monitored using UV−vis spectroscopy, which showed the formation of **2** (Supporting Information, ES, Figure S14). The generation of the initial Co^{III}-peroxo suggests that the NOD product has an ionizable/solvable NO_3^- anion, as observed in one of our previous report.[10a]

Scheme 2

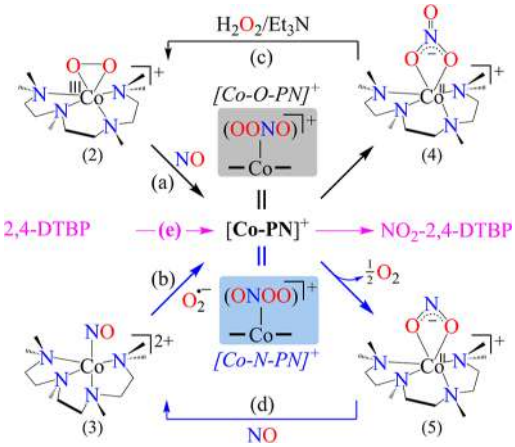

NOM Reaction of Co-Nitrosyl Complex {CoNO}^{8} (3). To understand the effect of the mode of coordinating species, we explored the reaction of **3** with $O_2^{\bullet-}$, an isoelectronic reaction system $[Co^{III}\text{−}O_2^{2-}$ + NO (total e^- count = **57**) = $\{CoNO\}^8 + O_2^{\bullet-}$ (total e^- count = **57**)] to the **2** + NO. In the NOO reaction of **3** with $O_2^{\bullet-}$, we observed the generation of **5**. The characteristic UV−vis absorption bands of **3** (λ_{max} = 330 nm) transformed to a new band (λ_{max} = 350 nm) within 20 min in CH_3CN at −40 °C under Ar (Figure 3a; Supporting Information, Figure S15). Complex **5** was characterized to be $[(HMTETA)Co^{II}(NO_2^-)]^+$ (NOM product) with the help of various spectroscopic tools, along with its structure using single-crystal X-ray diffraction (Scheme 2, reaction b). The FT-IR spectra of **5** showed a distinct peak for NO_2^- stretching at 1270 cm^{-1}, which changed to 1246 cm^{-1} ($^{15}NO_2^-$) when the reaction was performed using ^{15}N-labeled $\{Co^{15}NO\}^8$ and $O_2^{\bullet-}$ (inset: Figure 4a, Supporting Information, Figure S16a,b). This shifting of 24 cm^{-1} undoubtedly supports that the NO_2^- moiety's N-atom is derived from the NO ligand of **3**. The ESI-MS spectrum of the above reaction mixture showed a distinct peak at *m*/*z* 335.17, $[(HMTETA)Co^{II}(^{14}NO_2^-)]^+$ (calcd *m*/*z* 335.17) (Figure 4b), and shifted to 336.12, $[(HMTETA)Co^{II}(^{15}NO_2^-)]^+$ (calcd *m*/*z* 336.12) (inset: Figure 4b, Supporting Information, Figure S17). The ^{1}H NMR spectrum suggests a high-spin Co^{II}-center (*S* = 3/2),

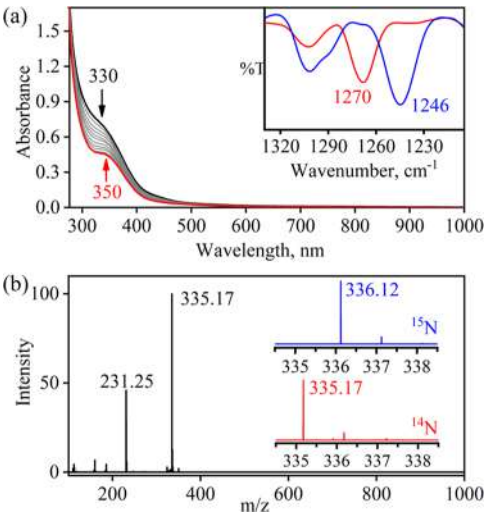

Figure 4. (a) Changes in the UV−vis spectra of **3** (0.1 mM, Black line) in the presence of $O_2^{\bullet-}$ under Ar at −40 °C in CH_3CN. In this reaction, black line (**3**) changed to a red line (**5**). Inset: FT-IR spectra **5**-$^{14}NO_2^-$ (red line) and **5**-$^{15}NO_2^-$ (blue line) recorded in KBr. (b) We observed a peak at 335.17, assigned to $[(HMTETA)\text{-}Co^{II}(NO_2^-)]^+$ (calcd *m*/*z* 335.17) in the ESI-MS spectrum of **5**. Isotopic distribution patterns for **5**-$^{14}NO_2^-$ (red line) and **5**-$^{15}NO_2^-$ (blue line) are shown in the Inset.

confirmed using the Evans method, and showed a 3.95 BM magnetic moment (Supporting Information, ES, Figure S18). Using Griess reagent, the yield of NO_2^- formed in the reaction mixture was calculated to be 92 (±2) % (Supporting Information, ES, Figure S19). The UV−vis spectrum of the isolated product of the reaction mixture of **3** + $O_2^{\bullet-}$ was compared with an authentic sample (prepared from **1** + NO_2^-), confirming the formation of **5** (Supporting Information, ES, Figure S20). Finally, the structural arrangement of the different atoms in **5** was determined by its single-crystal X-ray diffraction, which showed a distorted octahedral geometry around the Co-center (Figure 5a, Supporting Information, ES, Figure S21, and Tables T1 and T2).[10a,22a,c] The structure clearly shows that the bond length of the Co−O1 (2.205 Å) and Co−O2 (2.131 Å) suggests a different mode of coordination.

Dioxygen was determined as the side product in the reaction of **3** with $O_2^{\bullet-}$ and believed to be formed via a proposed transient *N*-bound $[Co\text{-}N\text{-}PN]^+$ intermediate (Scheme 2, reaction b). To confirm O_2 formation, we followed it using the gas-mass analyser for the reaction of **3** with $^{16}O_2^{\bullet-}$ from the headspace of the reaction flask and observed the formation of $^{16}O_2$ (Figure 5b), suggesting a presumed metal-PN intermediate as reported Cu^{II}−PN,[17,19c,27] Co^{II}−PN,[11b] and in aqueous PN chemistry.[28] Formation of O_2 from Co^{II}−PN might follow a couple of steps (Scheme 3), as discussed by Karlin and co-workers.[11b] As discussed above, the reaction of **3** with $O_2^{\bullet-}$ should proceed via a PN intermediate. To further confirm that the O_2 is not generated via the decomposition of $O_2^{\bullet-}$, we performed two control experiments, i.e., the reaction of **3** with (i) $^{18}O_2^{\bullet-}$ and (ii) $^{16}O_2^{\bullet-}/^{18}O_2^{\bullet-}$ (1:1). In these reactions, we observed the formation of a significant amount of (i) $^{18}O_2$ (Figure 5c) and (ii) a mixture of $^{18}O_2$ + $^{18}O^{16}O$ + $^{16}O_2$ (Figure 5d), respectively. Furthermore, the yield of O_2 was calculated by GC-mass analysis of the head space gas of the reaction sample vial and found to be 30%. We could not

https://doi.org/10.1021/acs.inorgchem.3c00639
Inorg. Chem. 2023, 62, 7385−7392

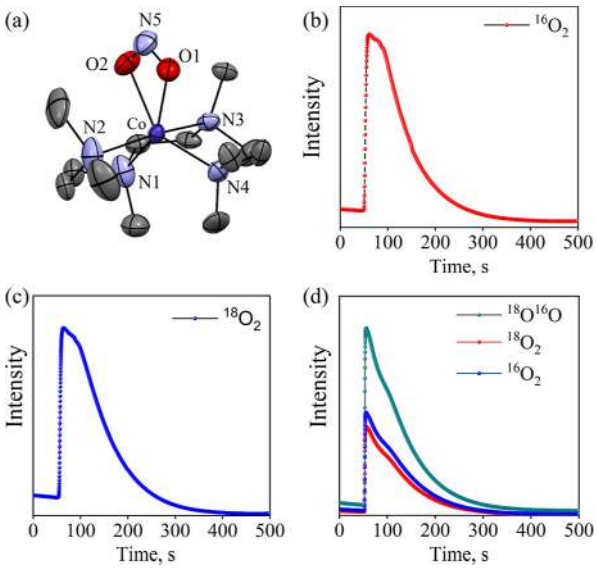

Figure 5. (a) Displacement ellipsoid plot of **5** (40% probability) at determined at 100 K. H-atoms and the anion have been removed for clarity. (b) Time-dependent formation of $^{16}O_2$ in the reaction of **3** (15.0 mM) with $^{16}O_2^{\bullet-}$ in CH_3CN at −40 °C followed by the gas-mass analyzer. (c) Time-dependent formation of $^{18}O_2$ in the reaction of **3** (15.0 mM) with $^{18}O_2^{\bullet-}$ in CH_3CN at −40 °C followed by the gas-mass analyzer. (d) Time-dependent formation of $^{18}O^{16}O/^{16}O_2/^{18}O_2$ in the reaction of **3** (15.0 mM) with $^{18}O_2^{\bullet-}/^{16}O_2^{\bullet-}$ (in 1:1 ratio) in CH_3CN at −40 °C followed by the gas-mass analyzer.

Scheme 3

$$[Co^{II}\text{-}\overset{O}{\overset{\|}{N}}\text{-}O\text{-}O]^+ \longrightarrow Co^{III}\text{-}O^{\bullet} + NO_2^-$$

$$Co^{III}\text{-}O^{\bullet} + [Co^{II}(NOOO)]^+ \longrightarrow Co^{III}\text{-}O\text{-}O^{\bullet} + [Co^{II}(NO_2^-)]^+$$

$$Co^{III}\text{-}O\text{-}O^{\bullet} \longrightarrow Co^{II} + O_2$$

$$Co^{II} + NO_2^- \longrightarrow [Co^{II}(NO_2^-)]^+$$

$$2[Co^{II}(NOOO)]^+ \longrightarrow 2[Co^{II}(NO_2^-)]^+ + O_2$$

follow the proposed $[Co\text{-}N\text{-}PN]^+$ spectroscopically; however, indirectly confirmed by the DTBP ring-nitration test.[10a] Also, exploring the same reaction in the presence of TBACl showed a higher yield of NO_2-2,4-DTBP [~75 (±2) %], supporting the PN moiety release from Co-center (Supporting Information, ES).[19c] The formation of NO_2-2,4-DTBP in sufficient amounts (Supporting Information, Figure S22) demonstrates the proposed $[Co\text{-}N\text{-}PN]^+$ intermediate in the reactions of **3** with $O_2^{\bullet-}$ (Scheme 2, reactions b and e). The above experimental finding supports our proposed mechanism of the generation of a proposed $[Co\text{-}N\text{-}PN]^+$ (Scheme 2, reaction b), which suggests the O−O bond homolytic cleavage in the PN intermediate, then O−O bond formation generating O_2 (Scheme 2, reaction b).[10a,11,16b,19c,k,26,28] These experiments confirm that the NOO reaction of **3** is a NOM reaction generating $Co^{II}-NO_2^-$ and 1/2 O_2 molecule as reported previously.[10a,11,16b,19c,k,26,28] This result is believed to follow the same reaction pathways as reported by Nam and co-workers, where a low spin $\{CoNO\}^8$ (S = 0) upon reaction with $O_2^{\bullet-}$ generated the $Co^{II}-NO_2^-$ + O_2 via the similar proposed $[Co\text{-}PN]^+$.[11] Even though the spin state of Co-center in **3** is S = 1, different from $\{CoNO\}^8$ (S = 0) reported by Nam and co-workers,[11] the NOO reaction was found to be independent of the spin state of the Co-center. Furthermore, we treated **5** with NO under Ar and followed the reaction with UV−vis measurements, showing the formation of **3** (Figure S23). This reaction confirms that the **5** has the ionizable/solvable NO_2^- anion, which in the presence of NO generates the $\{CoNO\}^8$ compound as observed in a previous report.[10a]

CONCLUSIONS

In this report, we have explored the NOO reactions of Co^{III}-peroxo, $[(HMTETA)Co^{III}(O_2)]^+$ ($Co^{III}-O_2^{2-}$, **2**), and Co-nitrosyl, $[(HMTETA)CoNO]^{2+}$ ($\{CoNO\}^8$, **3**), complexes bearing a common HMTETA ligand. As per the reports on *N*-bound and *O*-bound PN intermediate, the binding mode of the PN moiety with the metal center decides the transformation of PN to NO_3^- or NO_2^-.[10e,11b,15,16,19a−f,20a−c] Here, we observed that the NOO reaction of **2** leads to the formation of the NOD product, $Co^{II}-NO_3^-$ (**4**), and is supposed to proceed via the presumed [Co-*O*-PN] intermediate, similar to the NOD reactivity in the biological systems[7a] and observed in other examples.[10e,15,20] The O-coordinated [M-*O*-PN] (M = Fe, Co, Cu) are known to generate NO_3^-, as the same observed in the reaction of **2** + NO.[10e,15,20a−c] In contrast to NOD of **2**, the NOO reaction of **3** with $O_2^{\bullet-}$ produces the NOM product, $Co^{II}-NO_2^-$ (**5**), with O_2 evolution. NOM reaction of **3** possibly proceeds via the presumed *N*-coordinated [Co-*N*-PN] intermediate, as [M-*N*-PN] adduct produced from the M-NO ($\{FeNO\}^{7/8}$,$\{CoNO\}^{8/9}$) form M-NO_2^- + 1/2 O_2 and also observed in other examples.[11b,16,19a−f] Labeling experiments using $^{18}O_2^{\bullet-}$ and $^{16}O_2^{\bullet-}/^{18}O_2^{\bullet-}$ (1:1), undoubtedly support our proposed reaction sequences, where the O−O bond homolysis of PN moiety generates O_2, as reported in the earlier example.[10a,11,16b,19c,k,26,28] These reactions are believed to be regulated by the mode of the coordinating of PN in the $[M\text{-}PN]^+$ intermediates.[10e,11b,15,16,19a−f,20a−c] 2,4-DTBP ring nitration test supports the formation of proposed PN intermediate in the NOO reactions of **2** and **4**. Furthermore, the source of N-atom in $Co^{II}-NO_3^-$ (**4**) and $Co^{II}-NO_2^-$ (**5**) is derived from NO and supported by ^{15}N-labeling of ^{15}NO using FT-IR and mass spectrometry data. Observing two different products in the NOO reaction of $Co-O_2^{2-}$ and $\{CoNO\}^8$ bearing the same ligand framework is interesting. The mode of coordination and the isomerization of the proposed $[M\text{-}PN]^+$ intermediates' PN moieties are considered important in product determination.

ASSOCIATED CONTENT

Supporting Information

The Supporting Information is available free of charge at https://pubs.acs.org/doi/10.1021/acs.inorgchem.3c00639.

Experimental details, crystallographic data, single-crystal X-ray diffraction structures and their parameters, ^{1}H NMR of all compounds, ESI-mass spectra, additional FI-IR data, UV−vis absorption spectra, kinetics of reactivity, computed Eigen-value plot, and B3LYP/D2 optimized Cartesian coordinates (PDF)

Accession Codes

CCDC 2214926−2214928 contain the supplementary crystallographic data for this paper. These data can be obtained free of charge via www.ccdc.cam.ac.uk/data_request/cif, or by emailing data_request@ccdc.cam.ac.uk, or by contacting The

https://doi.org/10.1021/acs.inorgchem.3c00639
Inorg. Chem. 2023, 62, 7385−7392

Cambridge Crystallographic Data Centre, 12 Union Road, Cambridge CB2 1EZ, UK; fax: +44 1223 336033.

AUTHOR INFORMATION

Corresponding Author

Pankaj Kumar − *Department of Chemistry, Indian Institute of Science Education and Research (IISER), Tirupati 517507, India;* orcid.org/0000-0003-2530-7386; Email: pankajatiisert@gmail.com, pankaj@iisertirupati.ac.in

Authors

Kulbir − *Department of Chemistry, Indian Institute of Science Education and Research (IISER), Tirupati 517507, India;* orcid.org/0000-0001-8583-6920

Akshaya Keerthi C. S − *Department of Chemistry, Indian Institute of Science Education and Research (IISER), Tirupati 517507, India*

Sulthana Beegam − *Department of Chemistry, Indian Institute of Science Education and Research (IISER), Tirupati 517507, India*

Sandip Das − *Department of Chemistry, Indian Institute of Science Education and Research (IISER), Tirupati 517507, India;* orcid.org/0000-0002-4930-9071

Prabhakar Bhardwaj − *Department of Chemistry, Indian Institute of Science Education and Research (IISER), Tirupati 517507, India;* orcid.org/0000-0002-9987-8635

Mursaleem Ansari − *Department of Chemistry, Indian Institute of Technology (IIT), Bombay 400076, India*

Kuldeep Singh − *Department of Applied Chemistry, Amity University, Gwalior 474005, India;* orcid.org/0000-0002-2913-6644

Complete contact information is available at: https://pubs.acs.org/10.1021/acs.inorgchem.3c00639

Author Contributions

‖A.K.C.S. and S.B. contributed equally.

Notes

The authors declare no competing financial interest.

ACKNOWLEDGMENTS

This research was funded by SERB-DST grants (CRG/2021/003371 and EEQ/2021/000109). Kulbir, S.B., A.K.C.S., S.D., and P.B. would like to thank IISER Tirupati for providing the lab space and funding. The fellowship was provided by CRG/2021/003371 to A.K.C.S.

REFERENCES

(1) (a) Richter-Addo, G. B.; Legzdins, P.; Burstyn, J. Introduction: nitric oxide chemistry. *Chem. Rev.* **2002**, *102*, 857−860. (b) Bogdan, C. Nitric oxide and the immune response. *Nat. Immunol.* **2001**, *2*, 907−916. (c) Jia, L.; Bonaventura, C.; Bonaventura, J.; Stamler, J. S. S-nitrosohaemoglobin: a dynamic activity of blood involved in vascular control. *Nature* **1996**, *380*, 221−226. (d) Furchgott, R. F. Endothelium-Derived Relaxing Factor: Discovery, Early Studies, and Identifcation as Nitric Oxide (Nobel Lecture). *Angew. Chem., Int. Ed.* **1999**, *38*, 1870−1880. (e) Ignarro, L. J. Nitric oxide: a unique endogenous signaling molecule in vascular biology. *Biosci. Rep.* **1999**, *19*, 51−71. (f) Ignarro, L. J. *Nitric Oxide: Biology and Pathobiology*; Academic Press, 2000. (g) Lehnert, N.; Kim, E.; Dong, H. T.; Harland, J. B.; Hunt, A. P.; Manickas, E. C.; Oakley, K. M.; Pham, J.; Reed, G. C.; Alfaro, V. S. The Biologically Relevant Coordination Chemistry of Iron and Nitric Oxide: Electronic Structure and Reactivity. *Chem. Rev.* **2021**, *121*, 14682−14905.

(2) Li, H.; Förstermann, U. Uncoupling of endothelial NO synthase in atherosclerosis and vascular disease. *Curr. Opin. Pharmacol.* **2013**, *13*, 161−167.

(3) Wilcox, C. S. Oxidative stress and nitric oxide deficiency in the kidney: a critical link to hypertension? *Am. J. Physiol.: Regul., Integr. Comp. Physiol.* **2005**, *289*, R913−R935.

(4) Voetsch, B.; Jin, R. C.; Loscalzo, J. Nitric oxide insufficiency and atherothrombosis. *Histochem. Cell Biol.* **2004**, *122*, 353−367.

(5) (a) Castillo, L.; deRojas, T. C.; Chapman, T. E.; Vogt, J.; Burke, J. F.; Tannenbaum, S. R.; Young, V. R. Splanchnic metabolism of dietary arginine in relation to nitric oxide synthesis in normal adult man. *Proc. Natl. Acad. Sci. U.S.A.* **1993**, *90*, 193−197. (b) Palmer, R. M.; Ashton, D. S.; Moncada, S. Vascular endothelial cells synthesize nitric oxide from L-arginine. *Nature* **1988**, *333*, 664−666. (c) Liu, Q.; Gross, S. S. Binding sites of nitric oxide synthases. *Methods Enzymol.* **1996**, *268*, 311−324. (d) Nathan, C.; Xie, Q. W. Regulation of biosynthesis of nitric oxide. *J. Biol. Chem.* **1994**, *269*, 13725−13728.

(6) (a) Cosby, K.; Partovi, K. S.; Crawford, J. H.; Patel, R. P.; Reiter, C. D.; Martyr, S.; Yang, B. K.; Waclawiw, M. A.; Zalos, G.; Xu, X.; Huang, K. T.; Shields, H.; Kim-Shapiro, D. B.; Schechter, A. N.; Cannon, R. O., III; Gladwin, M. T. Nitrite reduction to nitric oxide by deoxyhemoglobin vasodilates the human circulation. *Nat. Med.* **2003**, *9*, 1498−1505. (b) Tsuchiya, K.; Kanematsu, Y.; Yoshizumi, M.; Ohnishi, H.; Kirima, K.; Izawa, Y.; Shikishima, M.; Ishida, T.; Kondo, S.; Kagami, S.; Takiguchi, Y.; Tamaki, T. Nitrite is an alternative source of NO in vivo. *Am. J. Physiol. Heart. Circ. Physiol.* **2005**, *288*, H2163−H2170.

(7) (a) Radi, R. Nitric oxide, oxidants, and protein tyrosine nitration. *Proc. Natl. Acad. Sci. U.S.A.* **2004**, *101*, 4003−4008. (b) Lim, C. H.; Dedon, P. C.; Deen, W. M. Kinetic analysis of intracellular concentrations of reactive nitrogen species. *Chem. Res. Toxicol.* **2008**, *21*, 2134−2147.

(8) (a) Gardner, P. R.; Gardner, A. M.; Martin, L. A.; Salzman, A. L. Nitric oxide dioxygenase: an enzymic function for flavohemoglobin. *Proc. Natl. Acad. Sci. U.S.A.* **1998**, *95*, 10378−10383. (b) Doyle, M. P.; Hoekstra, J. W. Oxidation of nitrogen oxides by bound dioxygen in hemoproteins. *J. Inorg. Biochem.* **1981**, *14*, 351−358. (c) Ford, P. C.; Lorkovic, I. M. Mechanistic aspects of the reactions of nitric oxide with transition-metal complexes. *Chem. Rev.* **2002**, *102*, 993−1018.

(9) (a) Collman, J. P.; Yang, Y.; Dey, A.; Decreau, R. A.; Ghosh, S.; Ohta, T.; Solomon, E. I. A functional nitric oxide reductase model. *Proc. Natl. Acad. Sci. U.S.A.* **2008**, *105*, 15660−15665. (b) Kurtz Jr, D. M. Flavo-diiron enzymes: nitric oxide or dioxygen reductases? *Dalton Trans.* **2007**, 4115−4121. (c) Lehnert, N.; Fujisawa, K.; Camarena, S.; Dong, H. T.; White, C. J. Activation of Non-Heme Iron-Nitrosyl Complexes: Turning Up the Heat. *ACS Catal.* **2019**, *9*, 10499−10518. (d) Pal, N.; Jana, M.; Majumdar, A. Reduction of NO by diiron complexes in relation to flavodiiron nitric oxide reductases. *Chem. Commun.* **2021**, *57*, 8682−8698.

(10) (a) Yenuganti, M.; Das, S.; Kulbir; Ghosh, S.; Bhardwaj, P.; Pawar, S. S.; Sahoo, S. C.; Kumar, P. Nitric oxide dioxygenation (NOD) reactions of Co^{III}-peroxo and Ni^{III}-peroxo complexes: NOD*versus*NO activation. *Inorg. Chem. Front.* **2020**, *7*, 4872−4882. (b) Kurtikyan, T. S.; Eksuzyan, S. R.; Hayrapetyan, V. A.; Martirosyan, G. G.; Hovhannisyan, G. S.; Goodwin, J. A. Nitric Oxide Dioxygenation Reaction by Oxy-Coboglobin Models: In-situ Low-Temperature FTIR Characterization of Coordinated Peroxynitrite. *J. Am. Chem. Soc.* **2012**, *134*, 13861−13870. (c) Yokoyama, A.; Cho, K. B.; Karlin, K. D.; Nam, W. Reactions of a chromium(III)-superoxo complex and nitric oxide that lead to the formation of chromium(IV)-oxo and chromium(III)-nitrito complexes. *J. Am. Chem. Soc.* **2013**, *135*, 14900−14903. (d) Yokoyama, A.; Han, J. E.; Cho, J.; Kubo, M.; Ogura, T.; Siegler, M. A.; Karlin, K. D.; Nam, W. Chromium(IV)−Peroxo Complex Formation and Its Nitric Oxide Dioxygenase Reactivity. *J. Am. Chem. Soc.* **2012**, *134*, 15269−15272. (e) Yokoyama, A.; Han, J. E.; Karlin, K. D.; Nam, W. An isoelectronic

NO dioxygenase reaction using a nonheme iron(III)-peroxo complex and nitrosonium ion. *Chem. Commun.* **2014**, *50*, 1742−1744.
(11) (a) Kumar, P.; Lee, Y. M.; Hu, L.; Chen, J.; Park, Y. J.; Yao, J.; Chen, H.; Karlin, K. D.; Nam, W. Factors That Control the Reactivity of Cobalt(III)-Nitrosyl Complexes in Nitric Oxide Transfer and Dioxygenation Reactions: A Combined Experimental and Theoretical Investigation. *J. Am. Chem. Soc.* **2016**, *138*, 7753−7762. (b) Kumar, P.; Lee, Y. M.; Park, Y. J.; Siegler, M. A.; Karlin, K. D.; Nam, W. Reactions of Co(III)-nitrosyl complexes with superoxide and their mechanistic insights. *J. Am. Chem. Soc.* **2015**, *137*, 4284−4287.
(12) Kurtikyan, T. S.; Eksuzyan, S. R.; Goodwin, J. A.; Hovhannisyan, G. S. Nitric Oxide Interaction with Oxy−Coboglobin Models Containing trans-Pyridine Ligand: Two Reaction Pathways. *Inorg. Chem.* **2013**, *52*, 12046−12056.
(13) Sharma, S. K.; Rogler, P. J.; Karlin, K. D. Reactions of a heme-superoxo complex toward a cuprous chelate and •NO(g): CcO and NOD chemistry. *J. Porphyr. Phthalocyanines* **2015**, *19*, 352−360.
(14) Saha, S.; Ghosh, S.; Gogoi, K.; Deka, H.; Mondal, B.; Mondal, B. Reaction of a Co(III)-Peroxo Complex and NO: Formation of a Putative Peroxynitrite Intermediate. *Inorg. Chem.* **2017**, *56*, 10932−10938.
(15) Hong, S.; Kumar, P.; Cho, K. B.; Lee, Y. M.; Karlin, K. D.; Nam, W. Mechanistic Insight into the Nitric Oxide Dioxygenation Reaction of Nonheme Iron(III)-Superoxo and Manganese(IV)-Peroxo Complexes. *Angew. Chem., Int. Ed. Engl.* **2016**, *55*, 12403−12407.
(16) (a) Mazumdar, R.; Mondal, B.; Saha, S.; Samanta, B.; Mondal, B. Reaction of a {Co(NO)}8 complex with superoxide: Formation of a six coordinated [CoII(NO)(O2−)] species followed by peroxynitrite intermediate. *J. Inorg. Biochem.* **2022**, *228*, 111698. (b) Gogoi, K.; Saha, S.; Mondal, B.; Deka, H.; Ghosh, S.; Mondal, B. Dioxygenation Reaction of a Cobalt-Nitrosyl: Putative Formation of a Cobalt-Peroxynitrite via a {Co(III)(NO)(O2(-))} Intermediate. *Inorg. Chem.* **2017**, *56*, 14438−14445.
(17) Maiti, D.; Lee, D. H.; Narducci Sarjeant, A. A.; Pau, M. Y. M.; Solomon, E. I.; Gaoutchenova, K.; Sundermeyer, J.; Karlin, K. D.; Karlin, K. D. Reaction of a copper-dioxygen complex with nitrogen monoxide (*NO) leads to a copper(II)-peroxynitrite species. *J. Am. Chem. Soc.* **2008**, *130*, 6700−6701.
(18) Fujisawa, K.; Soma, S.; Kurihara, H.; Dong, H. T.; Bilodeau, M.; Lehnert, N. A cobalt-nitrosyl complex with a hindered hydrotris(pyrazolyl) borate coligand: detailed electronic structure, and reactivity towards dioxygen. *Dalton Trans.* **2017**, *46*, 13273−13289.
(19) (a) Clarkson, S. G.; Basolo, F. Reaction of some cobalt nitrosyl complexes with oxygen. *Inorg. Chem.* **1973**, *12*, 1528−1534. (b) Clarkson, S. G.; Basolo, F. Reactions of some cobalt nitrosyl complexes with oxygen. *J. Chem. Soc., Chem. Commun.* **1972**, 670−671. (c) Park, G. Y.; Deepalatha, S.; Puiu, S. C.; Lee, D. H.; Mondal, B.; Narducci Sarjeant, A. A.; del Rio, D.; Pau, M. Y. M.; Solomon, E. I.; Karlin, K. D.; Karlin, K. D. A peroxynitrite complex of copper: formation from a copper-nitrosyl complex, transformation to nitrite and exogenous phenol oxidative coupling or nitration. *J. Biol. Inorg. Chem.* **2009**, *14*, 1301−1311. (d) Fujisawa, K.; Soma, S.; Kurihara, H.; Ohta, A.; Dong, H. T.; Minakawa, Y.; Zhao, J.; Alp, E. E.; Hu, M. Y.; Lehnert, N. Stable Ferrous Mononitroxyl {FeNO}(8) Complex with a Hindered Hydrotris(pyrazolyl)borate Coligand: Structure, Spectroscopic Characterization, and Reactivity Toward NO and O2. *Inorg. Chem.* **2019**, *58*, 4059−4062. (e) Videla, M.; Roncaroli, F.; Slep, L. D.; Olabe, J. A. Reactivity of reduced nitroprusside, [Fe(CN)5NO*]-3-toward oxygen. *J. Am. Chem. Soc.* **2007**, *129*, 278−279. (f) Patra, A. K.; Afshar, R. K.; Rowland, J. M.; Olmstead, M. M.; Mascharak, P. K. Thermally Induced Stoichiometric and Catalytic O-Atom Transfer by a Non-Heme Iron(III)−Nitro Complex: First Example of Reversible-{Fe−NO}7↔FeIII-NO2 Transformation in the Presence of Dioxygen. *Angew. Chem. Int. Ed. Engl.* **2003**, *42*, 4517−4521. (g) Kumar, P.; Kalita, A.; Mondal, B. Nitric oxide sensors based on copper(II) complexes of N-donor ligands. *Inorg. Chim. Acta* **2013**, *404*, 88−96. (h) Kumar, P.; Kalita, A.; Mondal, B. Copper(II) complexes as turn on fluorescent sensors for nitric oxide. *Dalton Trans.* **2012**, *41*, 10543−10548. (i) Kumar, P.; Kalita, A.; Mondal, B. Reduction of copper(II) complexes of tridentate ligands by nitric oxide and fluorescent detection of NO in methanol and water media. *Dalton Trans.* **2011**, *40*, 8656−8663. (j) Kumar, P.; Kalita, A.; Mondal, B. Nitric oxide reactivity of Cu(II) complexes of tetra- and pentadentate ligands: structural influence in deciding the reduction pathway. *Dalton Trans.* **2013**, *42*, 5731−5739. (k) Kalita, A.; Kumar, P.; Mondal, B. Reaction of a copper(II)-nitrosyl complex with hydrogen peroxide: putative formation of a copper(I)-peroxynitrite intermediate. *Chem. Commun.* **2012**, *48*, 4636−4638.
(20) (a) Wick, P. K.; Kissner, R.; Koppenol, W. H. Synthesis and Characterization of Tris(tetraethylammonium) Pentacyanoperoxynitritocobaltate(III). *Helv. Chim. Acta* **2000**, *83*, 748−754. (b) Wick, P. K.; Kissner, R.; Koppenol, W. H. Hydrolysis and Photolysis of Tris(tetraethylammonium) Pentacyanoperoxynitritocobaltate(III): Evidence for a Novel Complex, Pentacyanonitratocobaltate(III). *Helv. Chim. Acta* **2001**, *84*, 3057−3062. (c) Kim, S.; Siegler, M. A.; Karlin, K. D. Peroxynitrite chemistry derived from nitric oxide reaction with a Cu(II)-OOH species and a copper mediated NO reductive coupling reaction. *Chem. Commun.* **2014**, *50*, 2844−2846. (d) Das, S.; Akshaya Keerthi, C. S.; Kulbir; Singh, S.; Roy, S.; Singh, R.; Ghosh, S.; Kumar, P.; Kumar, P. Exploring the nitric oxide dioxygenation (NOD) reactions of manganese-peroxo complexes. *Dalton Trans.* **2023**, DOI: 10.1039/d3dt00159h.
(21) (a) Cho, J.; Kang, H. Y.; Liu, L. V.; Sarangi, R.; Solomon, E. I.; Nam, W. Mononuclear nickel(ii)-superoxo and nickel(iii)-peroxo complexes bearing a common macrocyclic TMC ligand. *Chem. Sci.* **2013**, *4*, 1502−1508. (b) Du, J.; Xu, D.; Zhang, C.; Xia, C.; Wang, Y.; Sun, W. Synthesis, characterization, and reactivity of a side-on manganese(iii)−peroxo complex bearing a pentadentate amino-pyridine ligand. *Dalton Trans.* **2016**, *45*, 10131−10135. (c) Jo, Y.; Annaraj, J.; Seo, M. S.; Lee, Y.-M.; Kim, S. Y.; Cho, J.; Nam, W. Reactivity of a cobalt(III)-peroxo complex in oxidative nucleophilic reactions. *J. Inorg. Biochem.* **2008**, *102*, 2155−2159.
(22) (a) Das, S.; Kulbir; Ghosh, S.; Chandra Sahoo, S.; Kumar, P. Nitric oxide monooxygenation (NOM) reaction of cobalt-nitrosyl {Co(NO)}8 to CoII-nitrito {CoII(NO2−)}: base induced hydrogen gas (H2) evolution. *Chem. Sci.* **2020**, *11*, 5037−5042. (b) Das, S.; Kulbir; Ray, S.; Devi, T.; Ghosh, S.; Harmalkar, S. S.; Dhuri, S. N.; Mondal, P.; Kumar, P. Why intermolecular nitric oxide (NO) transfer? Exploring the factors and mechanistic aspects of NO transfer reaction. *Chem. Sci.* **2022**, *13*, 1706−1714. (c) Kulbir; Das, S.; Devi, T.; Goswami, M.; Yenuganti, M.; Bhardwaj, P.; Ghosh, S.; Chandra Sahoo, S.; Kumar, P. Oxygen atom transfer promoted nitrate to nitric oxide transformation: a step-wise reduction of nitrate -> nitrite -> nitric oxide. *Chem. Sci.* **2021**, *12*, 10605−10612.
(23) Cho, J.; Sarangi, R.; Kang, H. Y.; Lee, J. Y.; Kubo, M.; Ogura, T.; Solomon, E. I.; Nam, W. Synthesis, structural, and spectroscopic characterization and reactivities of mononuclear cobalt(III)-peroxo complexes. *J. Am. Chem. Soc.* **2010**, *132*, 16977−16986.
(24) Kulbir; Das, S.; Devi, T.; Ghosh, S.; Chandra Sahoo, S.; Kumar, P. Acid-induced nitrite reduction of nonheme iron(ii)-nitrite: mimicking biological Fe−NiR reactions. *Chem. Sci.* **2023**, *14*, 2935−2942.
(25) Puthiyaveetil Yoosaf, M.; Ghosh, S.; Narayan, Y.; Yadav, M.; Sahoo, S. C.; Kumar, P. Finding a new pathway for acid-induced nitrite reduction reaction: formation of nitric oxide with hydrogen peroxide. *Dalton Trans.* **2019**, *48*, 13916−13920.
(26) (a) Ramezanian, M. S.; Padmaja, S.; Koppenol, W. H. Nitration and Hydroxylation of Phenolic Compounds by Peroxynitrite. *Chem. Res. Toxicol.* **1996**, *9*, 232−240. (b) Schopfer, M. P.; Mondal, B.; Lee, D. H.; Sarjeant, A. A.; Karlin, K. D. Heme/O2/*NO nitric oxide dioxygenase (NOD) reactivity: phenolic nitration via a putative heme-peroxynitrite intermediate. *J. Am. Chem. Soc.* **2009**, *131*, 11304−11305. (c) Vandervliet, A.; Eiserich, J. P.; Oneill, C. A.; Halliwell, B.; Cross, C. E. Tyrosine Modification by Reactive Nitrogen Species: A Closer Look. *Arch. Biochem. Biophys.* **1995**, *319*, 341−349.

https://doi.org/10.1021/acs.inorgchem.3c00639
Inorg. Chem. 2023, 62, 7385−7392

(27) Babich, O. A.; Gould, E. S. Electron transfer, 151. Decomposition of peroxynitrite as catalyzed by copper(II). *Res. Chem. Intermed.* **2002**, *28*, 575−583.
(28) (a) Pfeiffer, S.; Gorren, A. C.; Schmidt, K.; Werner, E. R.; Hansert, B.; Bohle, D. S.; Mayer, B. Metabolic fate of peroxynitrite in aqueous solution. Reaction with nitric oxide and pH-dependent decomposition to nitrite and oxygen in a 2:1 stoichiometry. *J. Biol. Chem.* **1997**, *272*, 3465−3470. (b) Coddington, J. W.; Hurst, J. K.; Lymar, S. V. Hydroxyl Radical Formation during Peroxynitrous Acid Decomposition. *J. Am. Chem. Soc.* **1999**, *121*, 2438−2443. (c) Koppenol, W. H.; Bounds, P. L.; Nauser, T.; Kissner, R.; Ruegger, H. Peroxynitrous acid: controversy and consensus surrounding an enigmatic oxidant. *Dalton Trans.* **2012**, *41*, 13779−13787.

https://doi.org/10.1021/acs.inorgchem.3c00639
Inorg. Chem. 2023, 62, 7385−7392